

Stronger, Steadier & Superior: Geometric Consistency in Depth VFM Forges Domain Generalized Semantic Segmentation

Siyu Chen¹ Ting Han^{2†} Changshe Zhang³ Xin Luo¹ Meiliu Wu⁴ Guorong Cai¹ Jinhe Su^{1†}

¹ Jimei University, ² Sun Yat-sen University, ³ Xidian University, ⁴ University of Glasgow,

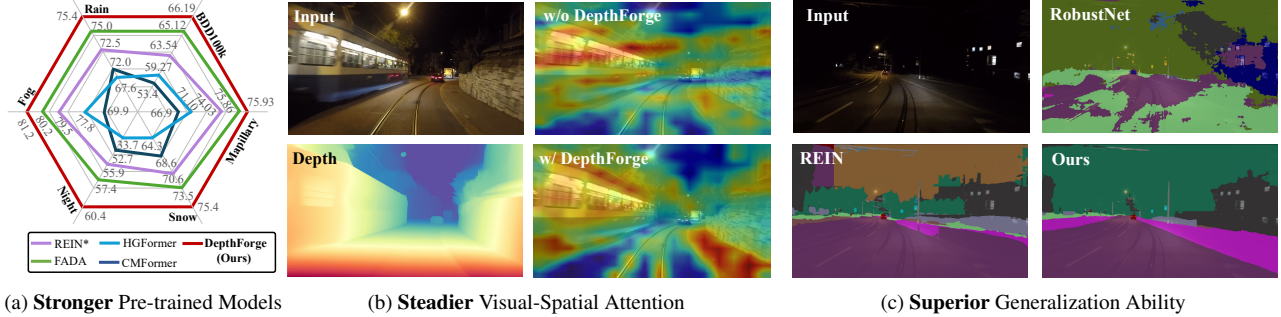


Figure 1. Existing methods fail to fully exploit the potential of VFMs for DGSS when visual cues are limited or absent. To this end, we introduce a novel and robust fine-tuning strategy **DepthForge** that leverages depth cues from a depth VFM to optimize visual cues, and employs spatial consistency to enhance feature discriminability. The proposed **DepthForge** achieves (a) **stronger** performance under extreme conditions, owing to (b) **steadier** visual-spatial attention, and thus delivers (c) **superior** generalization ability.

Abstract

Vision Foundation Models (VFMs) have delivered remarkable performance in Domain Generalized Semantic Segmentation (DGSS). However, recent methods often overlook the fact that visual cues are susceptible, whereas the underlying geometry remains stable, rendering depth information more robust. In this paper, we investigate **the potential of integrating depth information with features from VFMs**, to improve the geometric consistency within an image and boost the generalization performance of VFMs. We propose a novel fine-tuning DGSS framework, named **DepthForge**, which integrates the visual cues from frozen DINOv2 or EVA02 and depth cues from frozen Depth Anything V2. In each layer of the VFMs, we incorporate **depth-aware learnable tokens** to continuously decouple domain-invariant visual and spatial information, thereby enhancing depth awareness and attention of the VFMs. Finally, we develop a depth refinement decoder and integrate it into the model architecture to adaptively refine multi-layer VFM features and depth-aware learnable tokens. Extensive experiments are conducted based on various DGSS settings and five different datasets as unseen target domains. The qualitative and quantitative results demonstrate that our method significantly outperforms alternative approaches with **stronger performance, steadier visual-spatial attention, and superior generalization ability**. In particular,

DepthForge exhibits outstanding performance under extreme conditions (e.g., night and snow). Code is available at <https://github.com/anonymouse-xzrptkvyqc/DepthForge>.

1. Introduction

Domain Generalized Semantic Segmentation (DGSS) aims to improve prediction accuracy across multiple unseen domains without requiring access to their data, thereby ensuring robust generalization for practical applications [33, 44, 52]. One common approach involves decomposing the learned features into domain-invariant and domain-specific components [41, 46]. This method aims to achieve robustness against domain variations by isolating content-related factors from those that vary between domains. A second strategy employs meta-learning techniques [23], which focus on training models to generalize effectively across domains by learning more adaptable representations, often leveraging shared structures across different datasets.

Recently, VFMs have emerged as a promising approach, primarily owing to their strong generalization capabilities, which are enabled by pre-trained on large-scale datasets [14, 24, 35]. Fine-tuning these models has become increasingly popular due to their cost-effectiveness and superior performance [2, 43]. However, a significant challenge remains: *what constitutes robust feature information for do-*

main generalization, and how can such robust information be effectively extracted? Previous methods predominantly utilize VFMs based on RGB images. However, the inherent limitations of RGB prevent those methods from adapting to variable conditions, especially in scenarios such as nighttime, overexposure, snow, or fog, where visual cues are not clearly present. This clearly fails to meet the requirements of domain-generalized semantic segmentation.

In this paper, we introduce **DepthForge**, a robust fine-tuning and optimization strategy for domain generalization semantic segmentation, as shown in Fig. 1. Specifically, we employ two frozen VFMs: Depth Anything V2[48, 49] is dedicated to extract depth information, and DINOv2[29] or EVA02[14] are used to process RGB visual features. We enhance the generalization of the visual features at each layer of the VFMs by integrating the corresponding depth cues. More importantly, we introduce **depth-aware learnable tokens** that enable the model to learn spatial structure invariance, thereby ensuring consistent performance across different domains. The depth and visual features extracted from frozen VFMs are used to optimize the representation of our learnable tokens, thus producing more robust visual-spatial attention features than those based solely on visual cues and forging geometric consistency, as shown in Fig. 1(b). However, we observe that the frozen VFMs only provide static features, they are incapable of refining the feature maps during training. This limitation leads to persistent errors in the learnable tokens, causing the optimization process to drift in incorrect directions that are difficult to rectify. To this end, we propose a **depth refinement decoder** that dynamically adjusts the multi-scale features, combining prior features and dynamic features to establish high-quality paired feature relationships at different depth spaces.

The effectiveness of our design is verified by experiments on widely used Cityscapes, ACDC, Mapillary, BDD100k, and GTA5 datasets. In addition, the individual components of our design are also verified by extensive experiments. Extensive experiments have demonstrated that our method significantly improves DGSS performance, as shown in Fig. 1(c). Specifically, in the *GTA*→*Cityscapes* + *BDD100k* + *Mapillary* setting, we observed approximately **+4%** significant improvement in mIoU, particularly the improvement in extreme scenes is close to **+5%**. Our main contributions are summarized as follows:

- We propose a stronger DepthForge learning framework to fine-tune VFMs combined with visual and depth cues for domain-generalized semantic segmentation.
- A depth-awareness learnable tokens are introduced to focus on spatial relationship that acquires steadier and more robust visual-spatial attention. This strategy enables DepthForge to enhance the discriminability and refine features at an instance level within each layer.

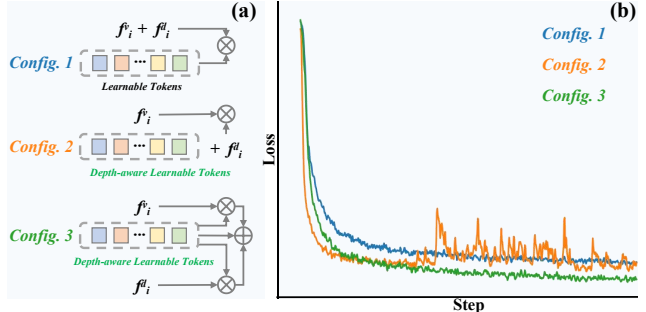


Figure 2. Different configurations of incorporating depth cues into visual information, where **Config.1:** adding f_i^d to f_i^v , or **Config.2:** incorporating f_i^d into the learnable token T_i , and **Config.3:** our DepthForge, respectively.

- Depth Forge highlights the impressive generalization ability, surpassing existing DGSS methods by a large margin, especially in extreme scenes with limited and absent visual cues.

2. Related Work

2.1. Domain Generalized Semantic Segmentation

Domain Generalized Semantic Segmentation (DGSS) aims to enhance the generalization capability of segmentation models to unseen domains. Recent methods primarily focus on reducing feature distribution discrepancies across domains and learning more domain-invariant representations. Adversarial training [52], meta-learning [4, 40], and self-supervised learning [17, 55] have been extensively explored to improve generalization performance. However, these methods often rely on constructing cross-domain contrastive constraints or employing sophisticated training strategies, limiting their generalization improvements and complicating the training process. The emergence of Vision Foundation Models (VFMs), trained via large-scale image-text [35] or image-image contrastive learning [29], has opened a promising avenue for DGSS. VFMs capture universal and rich visual representations beneficial for reducing domain biases. Recent approach [2, 43] leverages pre-trained VFMs by employing their frozen features as powerful generalized backbones to extract and refine learnable tokens, leading to significant improvements in model performance. Nevertheless, current DGSS approaches predominantly utilize RGB-only data, leaving the models susceptible to variations in lighting, texture, and spatial arrangements across different domains, thus constraining their full potential for generalization.

2.2. RGB-D Segmentation

Combining RGB with depth information has shown substantial benefits across various visual tasks [6, 8, 16, 38]. In object detection, RGB-D effectively mitigates limitations inherent to RGB data under complex scenes by providing

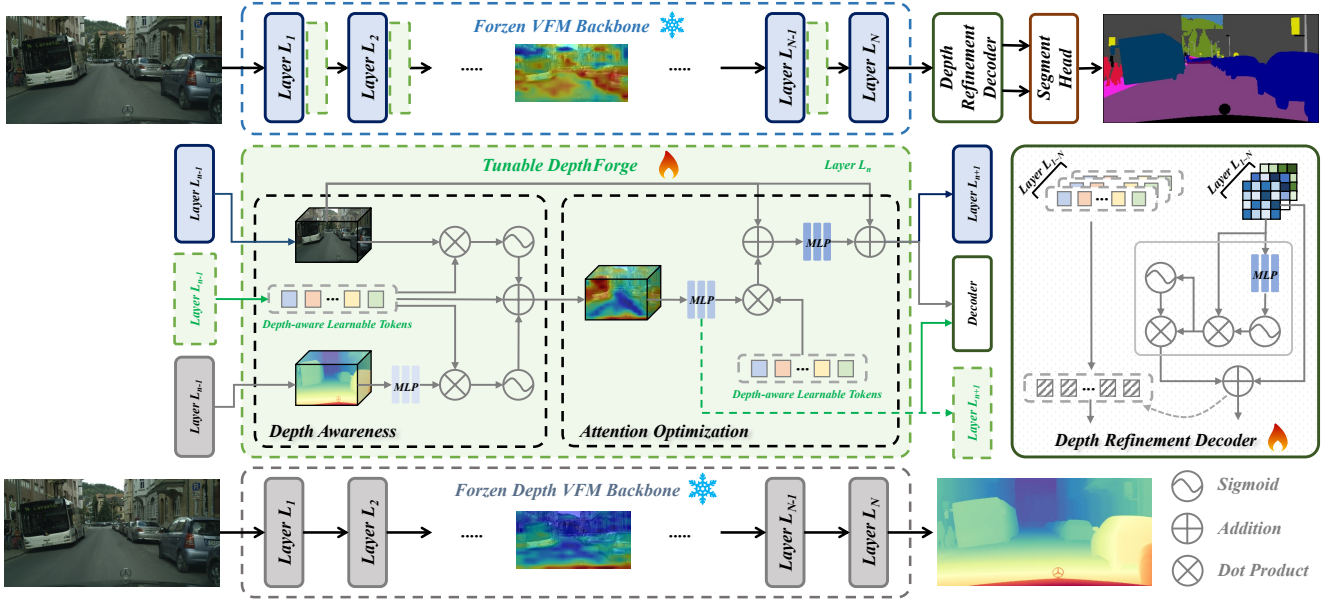


Figure 3. DepthForge framework. It incorporates the features from frozen VFM and depth VFM into our **Depth-aware Learnable Tokens** to generate enhanced features $f_{i+1} = f_i^v + \text{DepthForge}(f_i^v, f_i^d)$ for each layer. In our tunable DepthForge, We first design a Depth Awareness module that integrates visual and depth cues into learnable tokens. Next, we propose an Attention Optimization module to strengthen the discriminability of instances across different spatial locations. Finally, multi-scale features are fused in Depth refinement Decoder to adapt to various scales and spatial contexts. **Our DepthForge establishes direct connections to different instances in real-world locations, facilitating both feature refinement and improved discriminability.**

robust geometric and spatial cues, thereby enhancing localization accuracy and model robustness [42, 58]. In semantic segmentation, depth information assists models in capturing spatial structures and geometric contours of objects, alleviating issues related to imprecise object boundary delineation. Particularly in scenarios with blurred boundaries, insufficient illumination, or texture scarcity, the incorporation of depth information substantially improves segmentation accuracy and stability [13, 47, 53, 59]. Recent studies have further indicated that even in domain generalization tasks, integrating RGB and depth features consistently improves the model’s generalization performance on unseen domains [18, 26, 37, 54]. Therefore, exploring the integration of depth information to address the limitations of RGB-only approaches represents a promising and essential research direction within DGSS.

3. Preliminary

To achieve better generalization performance, existing approaches opt to fine-tune VFMs in a parameter-efficient manner. One mainstream idea is to refine and propagate features from frozen VFM layers to subsequent ones. Specifically, given a pre-trained VFM composed of N sequential layers $\{L_1, L_2, \dots, L_N\}$, where each layer is associated with a weight matrix $W_i \in \mathbb{R}^{c \times c}$ and the frozen output features of each layer are denoted as f_i for $i = 1, 2, \dots, N$. If we have a learnable weight matrix as $\Delta W_i \in \mathbb{R}^{c \times c}$, the feature

propagation from layer L_i to L_{i+1} is then formulated as:

$$f_{i+1} = W_i f_i + \Delta W_i f_i. \quad (1)$$

Recent REIN transfers the learnable matrix ΔW_i into a learnable token T_i :

$$f_{i+1} = W_i f_i + \epsilon(T_i(W_i f_i)), \quad (2)$$

where $\epsilon(\cdot)$ denotes the MLP function, and $T_i \in \mathbb{R}^{m \times c}$ with a token length m . REIN enables each token to connect better with instances in an image. However, we observe that since the updated and frozen features are limited to remain similar, this correlation is fragile and the capacity for feature refinement is limited.

This prompted us to explore **what kind of information could improve discrimination in instances and refine the feature representations**. Drawing inspiration from multi-modal learning, we observe that depth features provide a spatial relationship bias for corresponding pixels in visual features, thereby compensating for the loss of crucial visual cues in DGSS. We assume that incorporating a pre-trained depth VFM into the pre-trained VFMs will alleviate attention bias and significantly enhance scene understanding, particularly under extreme conditions.

We use the frozen features f_i^v from VFM for visual embedding, and the frozen features f_i^d from depth VFM for depth embedding. A straightforward thought might simply add f_i^d to f_i^v , or incorporate f_i^d into the learnable token T_i ,

Method	Proc. & Year	Snow	Night	Fog	Rain
<i>ResNet based:</i>					
IBN [30]	ECCV2018	49.6	21.2	63.8	50.4
Itenorm [20]	CVPR2019	49.9	23.8	63.3	50.1
IW [31]	CVPR2019	47.6	21.8	62.4	52.4
RobustNet [9]	CVPR2021	49.8	24.3	64.3	56.0
WildNet [25]	CVPR2022	28.4	12.7	41.2	34.2
<i>Transformer based:</i>					
HGFormer [12]	CVPR2023	68.6	52.7	69.9	72.0
CMFormer [3]	AAAI2024	64.3	33.7	77.8	67.6
<i>VFM based:</i>					
REIN [43]	CVPR2024	70.6	55.9	79.5	72.5
FADA [2]	NeurIPS2024	73.5	57.4	80.2	75.0
DepthForge(Ours)	-	75.4	60.4	81.2	75.4

Table 1. Performance comparison between our DepthForge and existing DGSS methods under *Citys. → ACDC with Snow, Night, Fog, Rain* generalization setting. Top three results are highlighted as **best**, **second**, and **third**, respectively. (%)

However, these methods lack flexibility and introduce significant inter-layer feature differences that prevent convergence, as shown in Fig. 2. In contrast, we propose **DepthForge** to adaptively fuse visual and depth cues, denoted as:

$$f_{i+1} = W_i^v f_i + \varepsilon(\epsilon^v(T_i(W_i^v f_i^v)) + \epsilon^d(T_i(W_i^d f_i^d))), \quad (3)$$

where W_i^v and W_i^d represent the weight matrix from VFMs and depth VFM, respectively. ε denote the adaptation of the visual and depth signals. This approach allows us to more effectively utilize the powerful capacities of multi-modal VFMs to forge robust refined features and instance discriminability.

More importantly, the depth VFM itself possesses strong generalization capabilities, allowing domain adaptation without fine-tuning. A pre-trained VFM applies the same. Therefore, the overall optimization objective still focuses on the segmentation head \mathcal{H} with parameter θ_h and our DepthForge with parameter θ_D :

$$\arg \min_{\theta_D, \theta_h} \sum_{i=1}^N \mathcal{L}oss(\mathcal{H}_{\theta_h}(\mathcal{F}_{\Theta^v, \Theta^d, \theta_D}(x_i)), y_i), \quad (4)$$

where x_i and y_i denote the input image and its corresponding ground truth, respectively, and N signifies the total number of images. \mathcal{F} represent the forward process of our DepthForge strategy applied to the pre-trained VFMs with parameters Θ^v and Θ^d .

4. DepthForge

This paper introduces the DepthForge strategy, a novel approach for domain generalized semantic segmentation. As

Method	Proc. & Year	BDD100k	Mapillary	GTA
<i>ResNet based:</i>				
IBN [30]	ECCV2018	48.56	57.04	45.06
Itenorm [20]	CVPR2019	49.23	56.26	45.73
IW [31]	CVPR2019	48.49	55.82	44.87
RobustNet [9]	CVPR2021	50.73	58.64	45.00
DRPC [51]	ICCV2019	49.86	56.34	45.62
GTR [32]	TIP2021	50.75	57.16	45.79
SHADE [56]	ECCV2022	50.95	60.07	48.61
SAW [34]	CVPR2022	52.95	59.81	47.28
WildNet [25]	CVPR2022	50.94	58.79	47.01
BlindNet [1]	CVPR2024	51.84	60.18	47.97
<i>Transformer based:</i>				
HGFormer [12]	CVPR2023	53.40	66.90	51.30
CMFormer [3]	AAAI2024	59.27	71.10	58.11
<i>VFM based:</i>				
REIN [43]	CVPR2024	63.54	74.03	62.41
FADA [2]	NeurIPS2024	65.12	75.86	63.78
DepthForge(Ours)	-	66.19	75.93	67.24

Table 2. Performance comparison between our **DepthForge** and existing DGSS methods under the *Citys. → BDD. + Map. + GTA5* generalization setting. Top three results are highlighted as **best**, **second**, and **third**, respectively. (%)

shown in Fig. 3, DepthForge consists of three main parts: (1) Depth Awareness; (2) Attention Optimization; (3) Depth Refinement Decoder. We detail the designs as follows.

4.1. Depth Awareness

Recent DGSS methods have applied pre-trained VFMs to source domain segmentation, with the core idea being to enhance the features between frozen VFM layers to help the model better adapt to target tasks. However, we observe that visual cues exhibit significant variations and even deficiencies across different scenes. Consequently, a more robust cue is required to provide a stronger prior for domain generalization. This motivates us to explore a strategy that focuses on the inherent similarities across different domains. In general, spatial location priors are able to help differentiate instances even when visual cues fail. To this end, we employ an additional depth VFM as an auxiliary network, as shown in Fig. 3.

Specifically, given a VFM \mathcal{V} and a depth VFM \mathcal{D} with N layers $\{L_1, L_2, \dots, L_N\}$, the corresponding features are denoted as $\{f_i^v, f_i^d | f_i \in \mathbb{R}^{n \times c}, i \in [1, N]\}$. Note that the layers $\{L_1, L_2, \dots, L_N\}$ are kept frozen. We acquire the visual feature f_i^v from the i -th layer L_i of \mathcal{V} , and the depth feature f_i^d from the corresponding layer of \mathcal{D} . Our goal is to generate the enhanced feature $\Delta f_i = \text{DepthForge}(f_i^v, f_i^d)$ by using both visual and depth cues.

We employ a set of learnable tokens $T = \{T_i \in \mathbb{R}^{m \times c} | i \in [1, N]\}$ to adaptively learn scene knowledge. As we consider, relying solely on visual cues can be limiting and prone to failure. Therefore, we utilize visual and depth

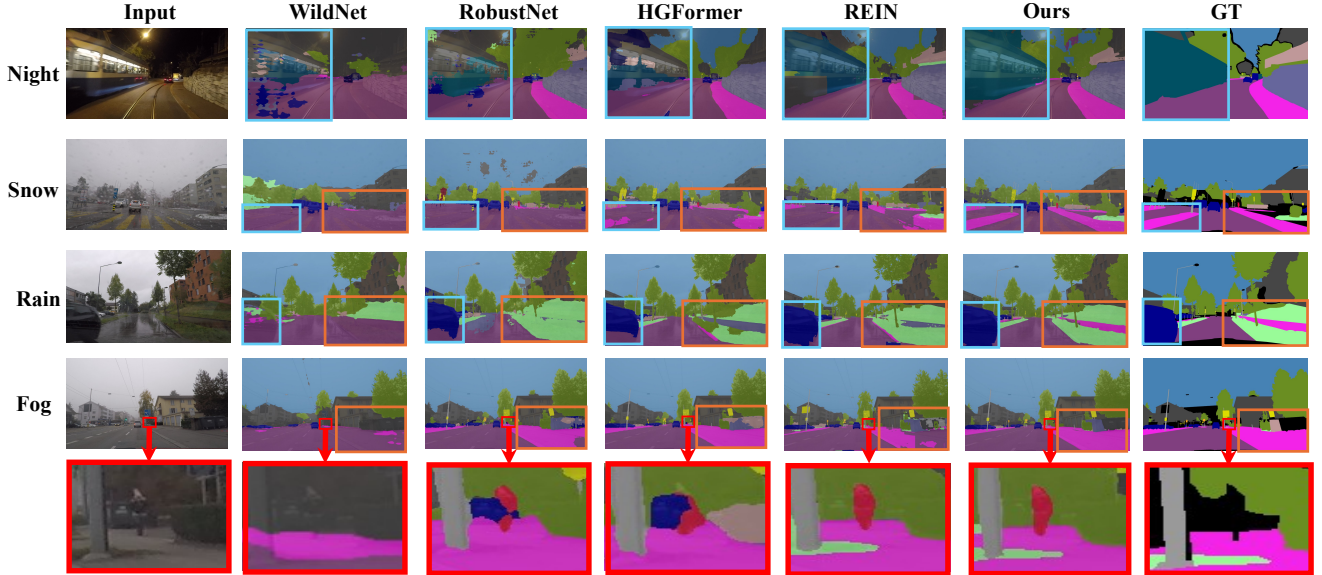


Figure 4. Key segmentation examples of existing DGSS methods and DepthForge under the Cityscapes to ACDC unseen target domains under Night, Snow, Rain, and Fog conditions.

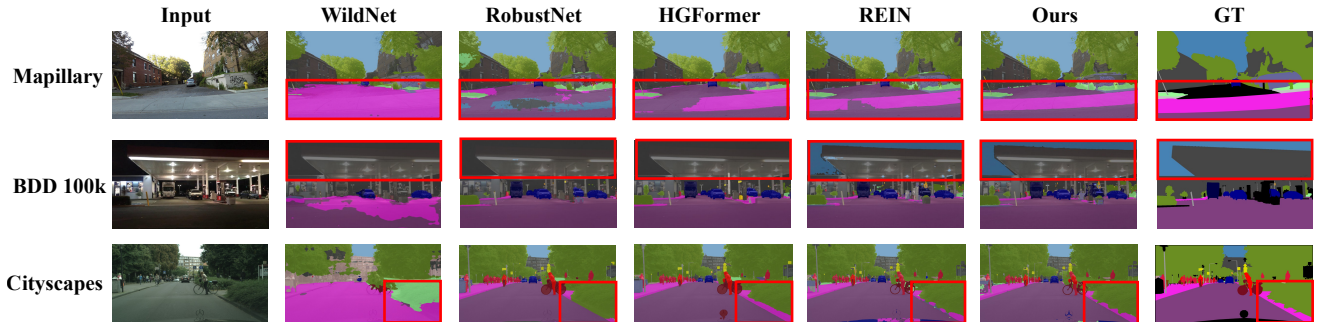


Figure 5. Key segmentation examples of existing DGSS methods and DepthForge under the GTA5 to Mapillary, BDD100k, and Cityscapes unseen target domains setting.

cues to construct learnable tokens, which we term depth-aware learnable tokens. We integrate T_i with f_i^v and f_i^d using an attention-based mechanism, prompting tailored adjustments to bridge the gap between source and target domains.

We use $f_i^{v,d}$ as the *query*, and T_i as the *key* and the *value*. A dot-product operation is applied to generate awareness map $A_i^{v,d}$, and the *Softmax* function is employed to align each patch with a unique instance:

$$A_i^{v,d} = \text{Softmax}\left(\frac{f_i^{v,d} \times T_i^\top}{\sqrt{c}}\right). \quad (5)$$

The $A_i^{v,d}$ provides insights into both the visual cues and depth retrieval, qualitatively evaluating the relationship between various tokens and visual or depth cues, respectively. Subsequently, we incorporate depth awareness bias A_i^d into the visual features A_i^v to provide additional spatial relationships, thereby establishing a latent connection between pix-

els and the real world. The process is mathematically formulated as $A_i = A_i^v + A_i^d$.

4.2. Attention Optimization

Directly leveraging the awareness representation A_i to generate enhanced features may introduce a significant amount of irrelevant information for downstream tasks. To this end, we employ depth-aware learnable tokens T_i to learn an alignment weight W_{T_i} and bias b_{T_i} . The T_i with weight W_{T_i} and bias b_{T_i} is then multiplied with the A_i to obtain the initial enhanced features $\hat{\Delta}f_i$ that embed both visual and depth cues, using the equation:

$$\hat{\Delta}f_i = A_i \times (T_i \times W_{T_i} + b_{T_i}), \quad (6)$$

where we select the same optimization strategy as REIN, discarding high-weight features when the features are sufficiently precise to avoid unnecessary adjustments and mitigate the risk of inappropriate variations. Finally, we employ

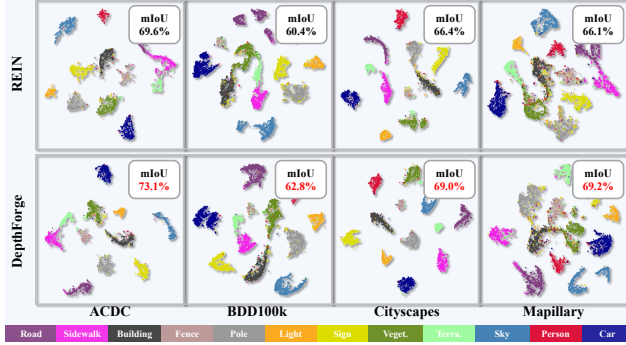


Figure 6. t-SNE visualization compares REIN and our **DepthForge**. The first volume corresponds to *Citys.* \rightarrow *ACDC*, and two through four volumes correspond to *GTA5* \rightarrow *BDD.* + *Citys.* + *Map.* The best mIoU results are highlighted in **red**.

two consecutive residual connections ϕ to enhance the flexibility of attention feature adjustment and prevent gradient vanishing during the forward pass. The calculation is defined as $\Delta f_i = \phi \hat{\Delta} f_i$. Benefiting from these depth-aware and attention optimization adjustments, DepthForge is capable of generating more distinctive, discriminative features for different categories within a single image, while balancing both visual and depth cues.

4.3. Depth Refinement Decoder

The depth-aware features at different layers are inconsistent. Therefore, how to design a robust decoder becomes a core challenge that effectively integrate these enhanced features across various scales to accomplish downstream tasks.

Previous methods rely solely on the output of the final layer f_N for semantic segmentation predictions. In contrast, we fuse the outputs from layers $L_1 - L_N$ to refine the depth features. Specifically, we process these multi-layer features with an MLP with two differnet fully-connected layers ϕ and φ and then concatenate them after a ReLU activation function:

$$f_i^{out} = \phi(\text{ReLU}(\varphi f_i)), \quad (7)$$

$$F_u = \gamma \text{Concat}(f_1^{out}, f_2^{out}, \dots, f_N^{out}), \quad (8)$$

where γ is a convolutional layer. Finally, we design several sequential multi-head Transformer layers to generate the final predictions.

5. Experiment

5.1. Datasets & Evaluation Protocols

We evaluate our DepthForge on four real-world datasets (Cityscapes [11], BDD100K [50], Mapillary [27], ACDC [39]) and a synthetic dataset (GTA5 [36]). **Cityscapes** (Citys.) is an autonomous driving dataset comprising 2,975

Method	Proc. & Year	Cityscapes	BDD100k	Mapillary
<i>ResNet based:</i>				
DRPC [51]	ICCV2019	37.42	32.14	34.12
GTR [32]	TIP2021	37.53	33.75	34.52
RobustNet [9]	CVPR2021	36.58	35.20	40.33
DIRL [45]	AAAI2022	41.04	39.15	41.60
SHADE [56]	ECCV2022	44.65	39.28	43.34
WildNet [25]	CVPR2023	44.62	38.42	46.09
SAW [34]	CVPR2022	39.75	37.34	41.86
AdvStyle [57]	NeurIPS2022	39.62	35.54	37.00
SPC [21]	CVPR2023	44.10	40.46	45.51
BlindNet [1]	CVPR2024	45.72	41.32	47.08
<i>Transformer based:</i>				
CMFormer [3]	AAAI2024	55.31	49.91	60.09
<i>VFM based:</i>				
DIDEX [28]	WACV2024	62.00	54.30	63.00
REIN [43]	CVPR2024	66.40	60.40	66.10
FADA [2]	NeurIPS2024	68.23	61.94	68.09
DepthForge(Ours)	-	69.04	62.82	69.22

Table 3. Performance comparison between our **DepthForge** and existing DGSS methods under the *GTA5* \rightarrow *Citys.* + *BDD.* + *Map.* generalization setting. Top three results are highlighted as **best**, **second**, and **third**, respectively. (%)

training images and 500 validation images, each with a resolution of 2048×1024 . **BDD100K** (BDD.) and **Mapillary** (Map.) provide 1,000 and 2,000 validation images, with resolutions of 1280×720 and 1902×1080 , respectively. **ACDC** offers 406 validation images captured under extreme conditions: namely at Night, Snow, Fog, and Rain, each with a resolution of 1902×1080 . **GTA5** is a synthetic dataset that provides 24,966 annotated images obtained from the game.

Following the evaluation protocol of the existing DGSS methods, a certain dataset is chosen as the source domain for training, and the other three datasets serve as unseen target domains for validation. The three common evaluation settings are as follows: (1) Cityscapes \rightarrow ACDC (Night, Snow, Fog, Rain); (2) GTA5 \rightarrow Cityscapes, BDD100K, Mapillary; and (3) Cityscapes \rightarrow BDD100K, Mapillary, GTA5. The evaluation metric is the mean Intersection-over-Union (mIoU).

5.2. Deployment Details & Parameter Settings

Our implementation is built on the MMSegmentation [10] codebase. For optimization, we employ AdamW optimizer with an initial learning rate of $1e-4$, a weight decay of 0.05, an epsilon of $1e-8$, and beta values of (0.9, 0.999). A OneCycleLR scheduler is applied over 50,000 total steps with a maximum learning rate of $1e-4$, featuring a warmup phase covering 10% of the training iterations, and using cosine annealing, with both the `div_factor` and `final_div_factor` set to 10.

Data augmentation includes multi-scale resizing, random cropping (with a fixed crop size and category ratio constraints), random flipping, and photometric distortion. All

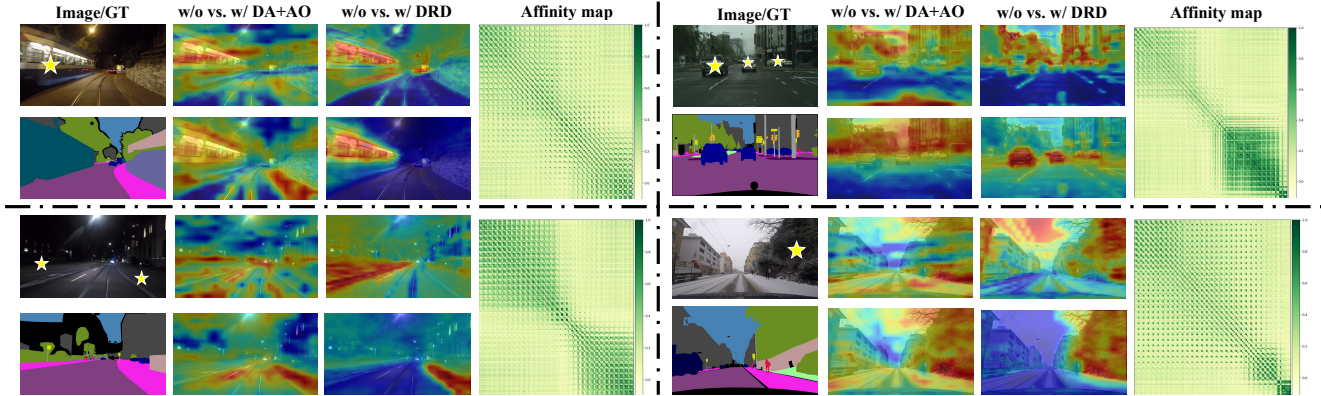


Figure 7. Visualizations of attention maps and affinity maps under different configurations, where DRD denotes the Depth Refinement Decoder, DA and AO represent the Depth Awareness and Attention Optimization, respectively.

Backbone	Configurations	Snow	Night	Fog	Rain	BDD	Map
EVA02 (Large) [14, 15]	REIN [43]	66.0	52.1	76.0	69.5	60.0	70.0
	+ concat f_i^d	66.3	52.2	76.2	69.8	60.2	70.2
	+ Prompt Depth Anything	65.8	52.4	75.5	69.3	60.4	69.9
	+ Depth Anything V2	67.2	53.0	77.0	70.2	60.9	70.8
	+ DRD	67.7	53.5	77.6	70.7	61.2	71.0
	+ DA + AO	67.9	53.7	77.8	70.9	61.5	71.2
	DepthForge	69.5	54.5	78.5	72.0	62.0	73.0
DINOv2 (Large) [29]	REIN [43]	70.6	55.9	79.5	72.5	63.5	74.0
	+ concat f_i^d	70.8	56.1	79.4	72.8	63.6	74.2
	+ Prompt Depth Anything	70.4	55.5	79.7	72.0	63.8	73.9
	+ Depth Anything V2	71.5	56.7	80.5	73.3	64.4	74.5
	+ DRD	72.0	57.2	80.7	74.0	64.9	74.8
	+ DA + AO	72.2	57.4	80.9	74.2	65.1	75.0
	DepthForge	75.4	60.4	81.2	75.4	66.2	76.0

Table 4. Ablation studies on component configurations of the proposed **DepthForge** under *Citys.* \rightarrow *ACDC* with *Snow*, *Night*, *Fog*, *Rain* + *BDD*. + *Map.* generalization setting, where DRD denotes the Depth Refinement Decoder, DA and AO represent the Depth Awareness and Attention Optimization. Top three results are highlighted as **best**, **second**, and **third**, respectively. (%)

experiments are conducted on an NVIDIA RTX 3090 GPU.

5.3. Comparison with State-of-The-Art Methods

We compare our approach with existing DGSS methods, including: (1) ResNet-based methods, (2) Transformer-based methods, and (3) VFM-based methods.

Cityscapes \rightarrow ACDC. Tab. 1 presents the performance on the Cityscapes source domain and the ACDC target domain. Compared with the VFM-based REIN and FADA, the proposed DepthForge shows mIoU improvement of 4.8% & 1.9%, 4.5% & 3.0%, 1.7% & 1.0%, and 2.9% & 0.4% for the Snow, Night, Fog, and Rain scenes, respectively. The feature space of the REIN and the proposed method is visualized in the first volume of Fig. 6. Moreover, our proposed method demonstrates superior performance compared to ResNet-based and Transformer-based approaches. These experimental results underscore the strong and robust generalization ability of DepthForge in extreme scenes with limited visual cues. Some exemplar segmentation results are compared under the Cityscapes \rightarrow ACDC are provided in Fig. 4. Our DepthForge shows better pixel-wise predic-

Backbone	Fine-tune Method	Trainable Params*	mIoU			
			Citys	BDD	Map	Avg.
CLIP [35] (ViT-Large)	Full	304.15M	51.3	47.6	54.3	51.1
	Freeze	0.00M	53.7	48.7	55.0	52.4
	REIN	2.99M	57.1	54.7	60.5	57.4
	FADA	11.65M	58.7	55.8	62.1	58.9
	DepthForge(Ours)	7.33M	59.7	57.0	63.5	60.0
SAM [24] (Huge)	Full	632.18M	57.6	51.7	61.5	56.9
	Freeze	0.00M	57.0	47.1	58.4	54.2
	REIN	4.51M	59.6	52.0	62.1	57.9
	FADA	16.59M	61.0	53.2	63.4	60.0
	DepthForge(Ours)	8.85M	63.3	55.5	65.1	61.3
EVA02 [14, 15] (Large)	Full	304.24M	62.1	56.2	64.6	60.9
	Freeze	0.00M	56.5	53.6	58.6	56.2
	REIN	2.99M	65.3	60.5	64.9	63.6
	FADA	11.65M	66.7	61.9	66.1	64.9
	DepthForge(Ours)	7.33M	68.0	61.7	67.5	65.7
DINOv2 [29] (Large)	Full	304.20M	63.7	57.4	64.2	61.7
	Freeze	0.00M	63.3	56.1	63.9	61.1
	REIN	2.99M	66.4	60.4	66.1	64.3
	FADA	11.65M	68.2	62.0	68.1	66.1
	DepthForge(Ours)	7.33M	69.0	62.8	69.2	67.0

Table 5. Performance comparison of the proposed **DepthForge** across multiple VFMs as backbones under the *GTA5* \rightarrow *Citys.* + *BDD.* + *Map.* generalization setting. Mark * denotes trainable parameters in backbones. Top three results are highlighted as **best**, **second**, and **third**, respectively. (%)

tions than previous methods, demonstrating the effectiveness and significance of depth awareness in our design.

Cityscapes \rightarrow BDD, Map, GTA5. Tab. 2 shows that the proposed DepthForge achieves the state-of-the-art performance, outperforming the REIN and FADA by 2.65% & 1.07%, 1.9% & 0.07%, and 3.12% & 1.13% on the BDD100k, Mapillary, and GTA unseen target domains, respectively. The proposed method achieves an improvement of approximately 10% compared to ResNet- and Transformer-based approaches.

GTA5 \rightarrow Citys, Map, BDD. As shown in Tab. 3, the proposed DepthForge achieves mIoU improvements of 2.64%, 2.42%, and 3.12% on the Cityscapes, BDD100k,

Backbone	Fine-tune Method	Trainable Params*	mIoU			Avg.
			Citys	BDD	Map	
EVA02 (Large) [14, 15]	Full	304.24M	62.1	56.2	64.6	60.9
	+AdvStyle [57]	304.24M	63.1	56.4	64.0	61.2
	+PASTA [5]	304.24M	61.8	57.1	63.6	60.8
	+GTR-LTR [32]	304.24M	59.8	57.4	63.2	60.1
	Freeze	0.00M	56.5	53.6	58.6	56.2
	+AdvStyle [57]	0.00M	51.4	51.6	56.5	53.2
	+PASTA [5]	0.00M	57.8	52.3	58.5	56.2
	+GTR-LTR [32]	0.00M	52.5	52.8	57.1	54.1
	+LoRA [19]	1.18M	55.5	52.7	58.3	55.5
	+AdaptFormer [7]	3.17M	63.7	59.9	64.2	62.6
+VPT [22]	3.69M	62.2	57.7	62.5	60.8	
+REIN [43]	2.99M	65.3	60.5	64.9	63.6	
+FADA [2]	11.65M	66.7	61.9	66.1	64.9	
+DepthForge(Ours)	7.33M	68.0	61.7	67.5	65.7	
DINOv2 (Large) [29]	Full	304.20M	63.7	57.4	64.2	61.7
	+AdvStyle [57]	304.20M	60.8	58.0	62.5	60.4
	+PASTA [5]	304.20M	62.5	57.2	64.7	61.5
	+GTR-LTR [32]	304.20M	62.7	57.4	64.5	61.6
	Freeze	0.00M	63.3	56.1	63.9	61.1
	+AdvStyle [57]	0.00M	61.5	55.1	63.9	60.1
	+PASTA [5]	0.00M	62.1	57.2	64.5	61.3
	+GTR-LTR [32]	0.00M	60.2	57.7	62.2	60.0
	+LoRA [19]	0.79M	65.2	58.3	64.6	62.7
	+AdaptFormer [7]	3.17M	64.9	59.0	64.2	62.7
+VPT [22]	3.69M	65.2	59.4	65.5	63.3	
+REIN [43]	2.99M	66.4	60.4	66.1	64.3	
+FADA [2]	11.65M	68.2	62.0	68.1	66.1	
+DepthForge(Ours)	7.33M	69.0	62.8	69.2	67.0	

Table 6. Performance comparison of the proposed **DepthForge** against other DGSS methods under the *GTA5* \rightarrow *Citys.* + *BDD.* + *Map.* generalization setting. Mark * denotes trainable parameters in backbones. Top three results are highlighted as **best**, **second**, and **third**, respectively. (%)

and Mapillary unseen target domains, respectively. The feature space of REIN and our DepthForge is visualized in Fig. 6, demonstrating the effectiveness of our depth-aware learnable tokens in the visual-spatial attention learning. In addition, we outperform the latest FADA by approximately 1% across all three target domains. Visual examples for qualitative comparison are given in Fig. 5.

5.4. Ablation Studies

Depth awareness and attention optimization are significant for depth-aware learnable tokens. We find that simply incorporating a spatial cue bias into the original learnable tokens ($+f_i^d$) makes almost no difference. However, when we transform the original learnable tokens into depth-aware learnable tokens using the DepthForge framework, we achieve an approximate 2% improvement in the target domains ACDC and Mapillary, as shown in Tab. 4. The depth-aware learnable tokens compensate for the shortcomings of visual cues and establish more robust visual-spatial attention. This conclusion is supported by qualitative visualizations in Fig. 7.

Depth refinement decoder facilitates the perception

of both visual and depth information. As shown in Tab. 4, we observe that depth refinement decoder integrates multi-scale information to enhance the expressive capacity of both the frozen VFM features and the enhanced features. With the incorporation of depth information, this optimization effect is further amplified. This conclusion is corroborated by qualitative visualizations in Fig. 7.

5.5. Generalization on Other Setting

To Different Depth VFMs. We evaluate the performance of the proposed DepthForge across different depth VFMs. Tab. 4 shows the relative spatial relationships derived from Depth Anything v2 outperform the absolute spatial cues provided by Prompt Depth Anything. We believe that what is more crucial in an image is the relative spatial relationship, which establishes connections among pixels and between pixels and the world. In contrast, absolute spatial information introduces significant discrepancies that can act as noise to visual cues.

To Different VFMs. We evaluate the generalization ability of the proposed DepthForge across different VFMs. Tab. 5 shows the superiority of DepthForge when embedded into these VFMs.

To Token Fine-Tuning Methods. We further compare the proposed method with some existing fine-tuning methods. As shown in Tab. 5, the proposed DepthForge outperforms these methods in all unseen target domains.

6. Conclusion

This paper presents the DepthForge framework, a novel approach for robust domain generalization semantic segmentation. We provide a detailed analysis of the challenges and limitations faced by existing methods. To this end, we propose DepthForge to integrate a pretrained depth VFM for fine-tuning. We design depth-aware learnable tokens to provide supplementary spatial cues to the visual features, thereby improving geometric consistency and enhancing the pixel discriminability. Moreover, we incorporate multi-layer enhanced features to effectively capture spatial correlations across various scales. Extensive experiments demonstrate the substantial potential of leveraging multi-modal VFMs in the field of DGSS, particularly under extreme conditions where visual cues are limited or missing, validating the effectiveness of our DepthForge in forging VFMs for DGSS.

Limitations. The proposed method increases the parameter count by approximately 4M compared to previous work, but DepthForge remains parameter-efficient to balance performance and efficiency. However, the incorporation of depth cues may cause interference between the two VFMs, and in the future, we need to consider a unified architecture to achieve an implicit and efficient fusion.

References

- [1] Woo-Jin Ahn, Geun-Yeong Yang, Hyun-Duck Choi, and Myo-Taeg Lim. Style blind domain generalized semantic segmentation via covariance alignment and semantic consistency contrastive learning. In *CVPR*, pages 3616–3626, 2024. 4, 6
- [2] Qi Bi, Jingjun Yi, Hao Zheng, Haolan Zhan, Yawen Huang, Wei Ji, Yuexiang Li, and Yefeng Zheng. Learning frequency-adapted vision foundation model for domain generalized semantic segmentation. *NeurIPS*, 37:94047–94072, 2024. 1, 2, 4, 6, 8
- [3] Qi Bi, Shaodi You, and Theo Gevers. Learning content-enhanced mask transformer for domain generalized urban-scene segmentation. In *AAAI*, pages 819–827, 2024. 4, 6
- [4] Manh-Ha Bui, Toan Tran, Anh Tran, and Dinh Phung. Exploiting domain-specific features to enhance domain generalization. In *NeurIPS*, pages 21189–21201. Curran Associates, Inc., 2021. 2
- [5] Prithvijit Chattopadhyay, Kartik Sarangmath, Vivek Vijaykumar, and Judy Hoffman. Pasta: Proportional amplitude spectrum training augmentation for syn-to-real domain generalization. In *ICCV*, pages 19288–19300, 2023. 8
- [6] Geng Chen, Qingyue Wang, Bo Dong, Ruitao Ma, Nian Liu, Huazhu Fu, and Yong Xia. Em-trans: Edge-aware multi-modal transformer for rgb-d salient object detection. *IEEE Transactions on Neural Networks and Learning Systems*, 36(2):3175–3188, 2024. 2
- [7] Shoufa Chen, Chongjian Ge, Zhan Tong, Jiangliu Wang, Yibing Song, Jue Wang, and Ping Luo. Adaptformer: Adapting vision transformers for scalable visual recognition. *NeurIPS*, 35:16664–16678, 2022. 8
- [8] Siyu Chen, Ting Han, Changshe Zhang, Jinhe Su, Ruisheng Wang, Yiping Chen, Zongyue Wang, and Guorong Cai. Hspformer: Hierarchical spatial perception transformer for semantic segmentation. *IEEE Transactions on Intelligent Transportation Systems*, 2025. 2
- [9] Sungha Choi, Sanghun Jung, Huiwon Yun, Joanne T Kim, Seungryong Kim, and Jaegul Choo. Robustnet: Improving domain generalization in urban-scene segmentation via instance selective whitening. In *CVPR*, pages 11580–11590, 2021. 4, 6
- [10] MMSegmentation Contributors. MMSegmentation: Openmmlab semantic segmentation toolbox and benchmark. <https://github.com/open-mmlab/mms Segmentation>, 2020. 6
- [11] Marius Cordts, Mohamed Omran, Sebastian Ramos, Timo Rehfeld, Markus Enzweiler, Rodrigo Benenson, Uwe Franke, Stefan Roth, and Bernt Schiele. The cityscapes dataset for semantic urban scene understanding. In *CVPR*, pages 3213–3223, 2016. 6
- [12] Jian Ding, Nan Xue, Gui-Song Xia, Bernt Schiele, and Dengxin Dai. Hgformer: Hierarchical grouping transformer for domain generalized semantic segmentation. In *CVPR*, pages 15413–15423, 2023. 4
- [13] Siqi Du, Weixi Wang, Renzhong Guo, Ruisheng Wang, and Shengjun Tang. Asymformer: Asymmetrical cross-modal representation learning for mobile platform real-time rgb-d semantic segmentation. In *CVPRW*, pages 7608–7615, 2024. 3
- [14] Yuxin Fang, Quan Sun, Xinggong Wang, Tiejun Huang, Xinlong Wang, and Yue Cao. Eva-02: A visual representation for neon genesis. *arXiv preprint arXiv:2303.11331*, 2023. 1, 2, 7, 8
- [15] Yuxin Fang, Wen Wang, Binhui Xie, Quan Sun, Ledell Wu, Xinggong Wang, Tiejun Huang, Xinlong Wang, and Yue Cao. Eva: Exploring the limits of masked visual representation learning at scale. In *CVPR*, pages 19358–19369, 2023. 7, 8
- [16] Ting Han, Siyu Chen, Chuanmu Li, Zongyue Wang, Jinhe Su, Min Huang, and Guorong Cai. Epurate-net: Efficient progressive uncertainty refinement analysis for traffic environment urban road detection. *IEEE Transactions on Intelligent Transportation Systems*, 2024. 2
- [17] Sivan Harary, Eli Schwartz, Assaf Arbelle, Peter Staar, Shady Abu-Hussein, Elad Amrani, Roei Herzig, Amit Alfassy, Raja Giryes, Hilde Kuehne, Dina Katabi, Kate Saenko, Rogerio Feris, and Leonid Karlinsky. Unsupervised domain generalization by learning a bridge across domains. In *CVPR*, pages 5270–5280, 2022. 2
- [18] Zongtao He, Liuyi Wang, Ronghao Dang, Shu Li, Qingqing Yan, Chengju Liu, and Qijun Chen. Learning depth representation from rgb-d videos by time-aware contrastive pre-training. *IEEE TCSVT*, 34(6):4143–4158, 2024. 3
- [19] Edward J Hu, Yelong Shen, Phillip Wallis, Zeyuan Allen-Zhu, Yuanzhi Li, Shean Wang, Lu Wang, and Weizhu Chen. Lora: Low-rank adaptation of large language models. *arXiv preprint arXiv:2106.09685*, 2021. 8
- [20] Lei Huang, Yi Zhou, Fan Zhu, Li Liu, and Ling Shao. Iterative normalization: Beyond standardization towards efficient whitening. In *CVPR*, pages 4874–4883, 2019. 4
- [21] Wei Huang, Chang Chen, Yong Li, Jiacheng Li, Cheng Li, Fenglong Song, Youliang Yan, and Zhiwei Xiong. Style projected clustering for domain generalized semantic segmentation. In *CVPR*, pages 3061–3071, 2023. 6
- [22] Menglin Jia, Luming Tang, Bor-Chun Chen, Claire Cardie, Serge Belongie, Bharath Hariharan, and Ser-Nam Lim. Visual prompt tuning. In *ECCV*, pages 709–727. Springer, 2022. 8
- [23] Jin Kim, Jiyoung Lee, Jungin Park, Dongbo Min, and Kwanghoon Sohn. Pin the memory: Learning to generalize semantic segmentation. In *CVPR*, 2022. 1
- [24] Alexander Kirillov, Eric Mintun, Nikhila Ravi, Hanzi Mao, Chloe Rolland, Laura Gustafson, Tete Xiao, Spencer Whitehead, Alexander C Berg, Wan-Yen Lo, et al. Segment anything. In *ICCV*, pages 4015–4026, 2023. 1, 7
- [25] Suhyeon Lee, Hongje Seong, Seongwon Lee, and Euntai Kim. Wildnet: Learning domain generalized semantic segmentation from the wild. In *CVPR*, pages 9936–9946, 2022. 4, 6
- [26] Zhiyu Liu, Munawar Hayat, Hong Yang, Duo Peng, and Yinjie Lei. Deep hypersphere feature regularization for weakly supervised rgb-d salient object detection. *IEEE TIP*, 32:5423–5437, 2023. 3
- [27] Gerhard Neuhold, Tobias Ollmann, Samuel Rota Buló, and Peter Kontschieder. The mapillary vistas dataset for semantic

- understanding of street scenes. In *ICCV*, pages 4990–4999, 2017. 6
- [28] Joshua Niemeijer, Manuel Schwonberg, Jan-Aike Termöhlen, Nico M Schmidt, and Tim Fingscheidt. Generalization by adaptation: Diffusion-based domain extension for domain-generalized semantic segmentation. In *Proceedings of the IEEE/CVF Winter Conference on Applications of Computer Vision*, pages 2830–2840, 2024. 6
- [29] Maxime Oquab, Timothée Darcet, Théo Moutakanni, Huy Vo, Marc Szafraniec, Vasil Khalidov, Pierre Fernandez, Daniel Haziza, Francisco Massa, Alaaeldin El-Nouby, et al. Dinov2: Learning robust visual features without supervision. *arXiv preprint arXiv:2304.07193*, 2023. 2, 7, 8
- [30] Xingang Pan, Ping Luo, Jianping Shi, and Xiaoou Tang. Two at once: Enhancing learning and generalization capacities via ibn-net. In *ECCV*, pages 464–479, 2018. 4
- [31] Xingang Pan, Xiaohang Zhan, Jianping Shi, Xiaoou Tang, and Ping Luo. Switchable whitening for deep representation learning. In *CVPR*, pages 1863–1871, 2019. 4
- [32] Duo Peng, Yinjie Lei, Lingqiao Liu, Pingping Zhang, and Jun Liu. Global and local texture randomization for synthetic-to-real semantic segmentation. *IEEE TIP*, 30: 6594–6608, 2021. 4, 6, 8
- [33] Duo Peng, Yinjie Lei, Munawar Hayat, Yulan Guo, and Wen Li. Semantic-aware domain generalized segmentation. In *CVPR*, pages 2584–2595, 2022. 1
- [34] Duo Peng, Yinjie Lei, Munawar Hayat, Yulan Guo, and Wen Li. Semantic-aware domain generalized segmentation. In *CVPR*, pages 2594–2605, 2022. 4, 6
- [35] Alec Radford, Jong Wook Kim, Chris Hallacy, Aditya Ramesh, Gabriel Goh, Sandhini Agarwal, Girish Sastry, Amanda Askell, Pamela Mishkin, Jack Clark, et al. Learning transferable visual models from natural language supervision. In *International conference on machine learning*, pages 8748–8763. PmLR, 2021. 1, 2, 7
- [36] Stephan R Richter, Vibhav Vineet, Stefan Roth, and Vladlen Koltun. Playing for data: Ground truth from computer games. In *ECCV*, pages 102–118. Springer, 2016. 6
- [37] Giulia Rizzoli, Donald Shenaj, and Pietro Zanuttigh. Source-free domain adaptation for rgb-d semantic segmentation with vision transformers. In *Proceedings of the IEEE/CVF Winter Conference on Applications of Computer Vision (WACV) Workshops*, pages 615–624, 2024. 3
- [38] Giulia Rizzoli, Donald Shenaj, and Pietro Zanuttigh. Source-free domain adaptation for rgb-d semantic segmentation with vision transformers. In *Proceedings of the IEEE/CVF Winter Conference on Applications of Computer Vision*, pages 615–624, 2024. 2
- [39] Christos Sakaridis, Dengxin Dai, and Luc Van Gool. Acdc: The adverse conditions dataset with correspondences for semantic driving scene understanding. In *ICCV*, pages 10745–10755, 2021. 6
- [40] Yang Shu, Zhangjie Cao, Chenyu Wang, Jianmin Wang, and Mingsheng Long. Open domain generalization with domain-augmented meta-learning. In *CVPR*, pages 9619–9628, 2021. 2
- [41] Zhiqiang Tang, Yunhe Gao, Yi Zhu, Zhi Zhang, Mu Li, and Dimitris Metaxas. Crossnorm and selfnorm for generalization under distribution shifts. In *ICCV*, 2021. 1
- [42] Jie Wang, Kechen Song, Yanqi Bao, Liming Huang, and Yunhui Yan. Cgfnet: Cross-guided fusion network for rgb-t salient object detection. *IEEE TCSVT*, 32(5):2949–2961, 2022. 3
- [43] Zhixiang Wei, Lin Chen, Yi Jin, Xiaoxiao Ma, Tianle Liu, Pengyang Ling, Ben Wang, Huaian Chen, and Jinjin Zheng. Stronger fewer & superior: Harnessing vision foundation models for domain generalized semantic segmentation. In *CVPR*, pages 28619–28630, 2024. 1, 2, 4, 6, 7, 8
- [44] Binhui Xie, Shuang Li, Mingjia Li, Chi Harold Liu, Gao Huang, and Guoren Wang. Sepico: Semantic-guided pixel contrast for domain adaptive semantic segmentation. *IEEE TPAMI*, 45(7):9004–9021, 2023. 1
- [45] Qi Xu, Liang Yao, Zhengkai Jiang, Guannan Jiang, Wenqing Chu, Wenhui Han, Wei Zhang, Chengjie Wang, and Ying Tai. Dirl: Domain-invariant representation learning for generalizable semantic segmentation. In *AAAI*, pages 2884–2892, 2022. 6
- [46] Qi Xu, Liang Yao, Zhengkai Jiang, Guannan Jiang, Wenqing Chu, Wenhui Han, Wei Zhang, Chengjie Wang, and Ying Tai. Dirl: Domain-invariant representation learning for generalizable semantic segmentation. In *AAAI*, page 2884–2892, 2022. 1
- [47] Jun Yang, Lizhi Bai, Yaoru Sun, Chunqi Tian, Maoyu Mao, and Guorun Wang. Pixel difference convolutional network for rgb-d semantic segmentation. *IEEE TCSVT*, 34(3):1481–1492, 2024. 3
- [48] Lihe Yang, Bingyi Kang, Zilong Huang, Xiaogang Xu, Jiashi Feng, and Hengshuang Zhao. Depth anything: Unleashing the power of large-scale unlabeled data. In *CVPR*, 2024. 2
- [49] Lihe Yang, Bingyi Kang, Zilong Huang, Zhen Zhao, Xiaogang Xu, Jiashi Feng, and Hengshuang Zhao. Depth anything v2. *NeurIPS*, 2024. 2
- [50] Fisher Yu, Haofeng Chen, Xin Wang, Wenqi Xian, Yingying Chen, Fangchen Liu, Vashisht Madhavan, and Trevor Darrell. Bdd100k: A diverse driving dataset for heterogeneous multitask learning. In *CVPR*, pages 2636–2645, 2020. 6
- [51] Xiangyu Yue, Yang Zhang, Sicheng Zhao, Alberto Sangiovanni-Vincentelli, Kurt Keutzer, and Boqing Gong. Domain randomization and pyramid consistency: Simulation-to-real generalization without accessing target domain data. In *ICCV*, pages 2100–2110, 2019. 4, 6
- [52] Xiangyu Yue, Zangwei Zheng, Shanghang Zhang, Yang Gao, Trevor Darrell, Kurt Keutzer, and Alberto Sangiovanni Vincentelli. Prototypical cross-domain self-supervised learning for few-shot unsupervised domain adaptation. In *CVPR*, pages 13834–13844, 2021. 1, 2
- [53] Jiaming Zhang, Huayao Liu, Kailun Yang, Xinxin Hu, Ruiping Liu, and Rainer Stiefelhagen. Cmx: Cross-modal fusion for rgb-x semantic segmentation with transformers. *IEEE Transactions on Intelligent Transportation Systems*, 24(12): 14679–14694, 2023. 3
- [54] Lu Zhang, Siqi Zhang, Xu Yang, Hong Qiao, and Zhiyong Liu. Unseen object instance segmentation with fully

- test-time rgb-d embeddings adaptation. In *2023 IEEE International Conference on Robotics and Automation (ICRA)*, pages 4945–4952, 2023. [3](#)
- [55] Xingxuan Zhang, Linjun Zhou, Renzhe Xu, Peng Cui, Zheyang Shen, and Haoxin Liu. Towards unsupervised domain generalization. In *CVPR*, pages 4900–4910, 2022. [2](#)
- [56] Yuyang Zhao, Zhun Zhong, Na Zhao, Nicu Sebe, and Gim Hee Lee. Style-hallucinated dual consistency learning for domain generalized semantic segmentation. In *ECCV*, pages 535–552. Springer, 2022. [4](#), [6](#)
- [57] Zhun Zhong, Yuyang Zhao, Gim Hee Lee, and Nicu Sebe. Adversarial style augmentation for domain generalized urban-scene segmentation. *NeurIPS*, 35:338–350, 2022. [6](#), [8](#)
- [58] Wujie Zhou, Yun Zhu, Jingsheng Lei, Jian Wan, and Lu Yu. Ccafnet: Crossflow and cross-scale adaptive fusion network for detecting salient objects in rgb-d images. *IEEE TMM*, 24: 2192–2204, 2022. [3](#)
- [59] Wujie Zhou, Yuxiang Xiao, Weiqing Yan, and Lu Yu. Cmpffnet: Cross-modal and progressive feature fusion network for rgb-d indoor scene semantic segmentation. *IEEE Transactions on Automation Science and Engineering*, 21(4):5523–5533, 2024. [3](#)